

# Why does bulk boundary correspondence fail in some non-hermitian topological models

Ye Xiong\*

*Department of Physics and Institute of Theoretical Physics ,  
Nanjing Normal University, Nanjing 210023, P. R. China  
National Laboratory of Solid State Microstructures,  
Nanjing University, Nanjing 210093, P. R. China*

Bulk boundary correspondence is crucial to topological insulator as it associates the boundary states (with zero energy, chiral or helical) to topological numbers defined in bulk. The application of this correspondence needs a prerequisite condition which is usually not mentioned explicitly: the boundaries themselves cannot alter the bulk states, so as to the topological numbers defined on them. In non-hermitian models with fractional winding number, we prove that such precondition fails and the bulk boundary correspondence is cut out. We show that, as eliminating the hopping between the boundaries to simulate the evolution of a system from the periodic boundary condition to the open boundary condition, exceptional points must be passed through and the topological structure of the spectrum has been changed. This makes the topological structures of a chain with open boundary totally different from that without the boundary. We also argue that such exotic behavior does not emerge when the open boundary is replaced by a domain-wall. So the index theorem can be applied to the systems with domain-walls but cannot be further used to those with open boundary.

## I. INTRODUCTION

In quantum mechanics of hermitian Hamiltonian, the degeneracy of the energy spectrum plays crucial role in the generation of nontrivial topological order, i.e., the nonzero (first kind of) Chern number is generated by the effective magnetic monopoles at the degenerate points in the parameter space<sup>1</sup>. In a recent year, some authors try to spread these ideas to the models with non-hermitian(NH) Hamiltonian<sup>2-8</sup>. Besides the topological phase that is smoothly extended from the hermitian cases<sup>5,9</sup>, the NH models can possess new topological phases stemming from a new kind of degenerate points, the *exceptional points* (EPs)<sup>10-18</sup>.

The discussions on the NH Hamiltonian started more than half a century ago and a special kind of NH models,  $\mathcal{PT}$ -symmetric models, has been studied both theoretically and experimentally<sup>13-15,19-52</sup>. EPs are the special points in a parameter space where the NH matrix ceases to be diagonalizable because of the coalescences of the eigenvalues and eigenstates. These properties can be illustrated by the following  $2 \times 2$  Jordan block reading as

$$H = \begin{pmatrix} 0 & 1 \\ r_0 e^{-ik} & 0 \end{pmatrix}. \quad (1)$$

The EP at  $r_0 = 0$  is the point where the two eigenvalues coalesce to 0 and the right eigenstates (left eigenstates) coalesce to  $(1, 0)^T$  ( $(0, 1)$ ). As there is only one eigenstate, the Jordan block cannot be diagonalized any more at the EP. Each EP can induce a square root singularity so that there are multiple square root branches in the parameter space around it. This can also be illustrated with the above toy matrix by taking a positive  $r_0$  and encircling the EP by varying  $k$  from 0 to  $2\pi$ . The two

eigenvalues read

$$E_{\pm} = \sqrt{r_0 e^{ik}}. \quad (2)$$

Due to the two branches in the complex plane induced by the square root, the eigenvalues that continuously varying with  $k$  will come back to their original values after  $4\pi$  period instead of the  $2\pi$  period for the matrix itself. This fact leads to the fractional winding number introduced in the previous articles<sup>7,8</sup>.

In the previous comment, we question that it is necessary to connect the square root branches with the fractional winding number in a topological language<sup>53</sup>. In this article, we further prove that there is no bulk-boundary correspondence in these NH models and the zero energy boundary states (ZEBSs) are caused by the fact that the Hamiltonian is right at (or exponentially close to) an EP when the boundary is open. This is different from the ZEBSs that are protected by the chiral symmetry in the traditional topological insulators. As the open boundary is accompanying with EP while a domain-wall does not, the index theorem presented in Ref. 8 can only be applied to the systems with domain-wall but cannot be further extended to the systems with open boundary condition (OBC). Besides that, many exotic properties emerge, i.e., *all* bulk states are changed from extended states to the exponentially localized states when the boundary condition is changed from periodic to open and the bulk state spectrum are also entirely changed during this process.

## II. MODELS AND RESULTS

We start this section with the toy matrix in Eq. 1 because it will illustrate many exotic features associated

with EP. Some of the methods used here can be applied to the general models. We will talk about two kinds of EPs. When the Hamiltonian is presented in the momentum space, the first kind of EPs is in the parameter space spanned by  $r_0$  and  $k$  in Eq. 1, where  $r_0$  is the hopping between the nearest neighboring unit cells and  $k$  is the wave-vector. While in the real space representation, the second kind of EPs is in another parameter space spanned by  $r$  and  $\phi$  in Eq. 3, where  $r$  is the hopping between the two ends of the chain and  $\phi$  is the phase added on this hopping. We hope that the readers will not be confused by these two kinds.

The toy matrix can be considered as an effective NH Hamiltonian in the momentum space for a 1-dimensional (1D) model. In the real space, we suppose that the model is composited by  $N$  unit cells so that the Hamiltonian in the real space reads as

$$H = \sum_{l=1}^N c_{l,A}^\dagger c_{l,B} + \sum_{l=1}^{N-1} r_0 c_{l,B}^\dagger c_{l+1,A} + r e^{i\phi} c_{N,B}^\dagger c_{1,A}, \quad (3)$$

where  $A$  and  $B$  label the two inequivalent lattice sites in a unit cell. Without loss of generality, we take  $r_0$  to be real and positive. The last term represents the hopping between the two ends. When  $r = r_0$  and  $\phi = 0$ , the translational symmetry restores and the spectrum can be grouped into two branches by  $E_{\pm}(k) = \pm\sqrt{r_0}e^{ik/2}$  with  $N$  discrete  $k$ . In Fig. 1 (a), we schematically show the eigenvalues on a circle in the complex plane and the colors are used to distinguish the two branches. For the sake of clarity in our next discussion, we relabel these eigenvalues along the circle counterclockwise by  $E_{\alpha}$ , where  $\alpha = 1, 2, \dots, 2N$ . Then we adjust  $\phi$  from 0 to  $2\pi$  continuously in Eq. 3. The  $2N$ th-root of the complex number implies that  $E_{\alpha}$  is continuously changed to  $E_{\alpha+1}$  and  $E_{2N}$  is changed to  $E_1$ . We want to emphasize that this pumping property is distinct from that in the hermitian case and our general discussions will be based on it. In Fig. 1, we schematically show this distinction.

Next, we consider the effect of boundary by decreasing  $r$  while varying  $\phi$  as usual. In Fig. 2, we show how the eigenvalues evolve with  $\phi$  in a  $N = 4$  chain when  $r = X^{2N}r_0$ . In the figure,  $X^{2N}$  is taken as 1,  $10^{-4}$ ,  $10^{-8}$  and 0, respectively. Actually, When  $r \neq r_0$ , Eq. 3 can still be mapped back to a translational symmetric matrix by a non-unitary transformation,

$$H \rightarrow V^{-1}HV, \quad (4)$$

with  $V = \text{diag}(1, X, X^2, \dots, X^{2N-1})$ . Here  $V$  is a matrix with only diagonal elements  $1, X, \dots, X^{2N-1}$ . After the transformation, the difference between the hopping amplitudes at the boundary and in the bulk is smeared out and the hoppings in bulk are rescaled by  $X$ . This is why that only the radius but not the shape of the circle is changed as  $r$  is decreasing. We also notice that the above transformation indicates that all the right eigenstates becomes exponentially localized on the left end of

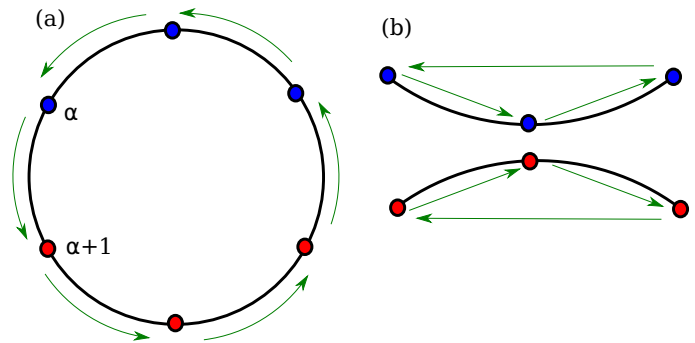


FIG. 1. (a) The alternation of eigenvalues when  $\phi$  is varying  $2\pi$  continuously in Eq. 3. As the translational symmetry is present in the case of  $\phi = n2\pi$ , the spectrum can be branched into  $E_{\pm}$ . Here the blue and red points represent the eigenvalues in these two branches, respectively. (b) For a typical hermitian Hamiltonian with two bands, inserting one quantum flux in the loop is equivalent to moving  $k$  by  $\frac{2\pi}{N}$  in the Brillouin zone. So the alternation of eigenvalues by varying  $\phi$  occurs within each band and is different from that in the NH case.

the chain while the left eigenstates localizes on the right end, which are confirmed by the numerical calculations.

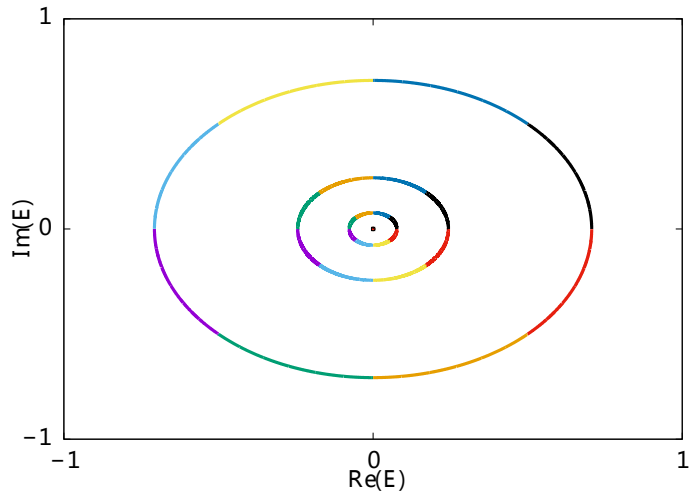


FIG. 2. (a) From outside to inside, the traces in different colors show how the eigenvalues vary with  $\phi$  in the complex plane when  $r = r_0, 10^{-4}r_0, 10^{-8}r_0$  and 0, respectively. The chain contains  $N = 4$  unit cells. So there are totally 8 eigenvalues, which are represented by different colors in the figure. As long as  $r \neq 0$ , one needs  $2N$  rounds of  $\phi$  to return to the initial eigenvalue sheet. Here  $r = 0$  is an EP, where all eigenstates coalesce together.

Here  $r = 0$  is an EP of the Hamiltonian in Eq. 3. Actually, this is a  $2N$  degenerate EP so that the  $2N$  eigenvalues coalesce to  $E = 0$ . All the right and the left eigenstates coalesce to  $(1, 0, \dots)^T$  and  $(0, \dots, 1)$ , respectively. And we need to encircle this EP (by taking  $r \neq 0$  and  $\phi = 0 \rightarrow 2\pi$ )  $2N$  rounds to reach the initial sheet of the eigenstates. One should note that in the momen-

tum space, the toy model is encircling an EP as varying  $k$  without touching any EP. But in the real space representation, when the OBC is taken, the model is right at an EP and the Hamiltonian matrix becomes defective. As the spectrum and the eigenstates are changed entirely in approaching OBC, we have to understand the ZEBs from the coalescence of eigenstates at the EP instead of the topological protection of boundary states caused by the bulk fractional winding numbers. One reason is that the bulk spectrum has been dramatically changed when the OBC is approached. This makes it impossible to connect the topological band structure in the momentum space to the boundary states in the real space because the two bulk spectra with and without OBC are totally different. So the index theorems, such as the Thouless pump<sup>54</sup>, cannot be applied any more. We will present the other reasons after the studies of several models.

In the momentum space, The 1D model in Ref. 7 is

$$H_k = (v + r_0 \cos(k))\sigma_x + (r_0 \sin(k) + i\gamma/2)\sigma_z. \quad (5)$$

After a unitary transformation  $U = \frac{1}{\sqrt{2}} \begin{pmatrix} 1 & 1 \\ i & -i \end{pmatrix}$ ,  $H_k \rightarrow U^\dagger H_k U$ , the Hamiltonian changes to

$$H_k = i \begin{pmatrix} 0 & (\gamma/2 - v) - r_0 e^{ik} \\ (\gamma/2 + v) + r_0 e^{-ik} & 0 \end{pmatrix}. \quad (6)$$

The EPs are at the points where either of the off-diagonal elements is zero. We first take  $\gamma = 1$ ,  $v = -0.5$  and  $r_0 = 0.5$ , which are in the topological phase with fractional winding number in Ref. 7. Similar to the toy model in the above discussion, we write down the Hamiltonian in the real space as

$$H = i \left\{ \sum_{l=1}^N c_{l,A}^\dagger c_{l,B} + \sum_{l=1}^{N-1} 1/2 [c_{l,B}^\dagger c_{l+1,A} - c_{l+1,A}^\dagger c_{l,B}] \right. \\ \left. + r [e^{i\phi} c_{N,B}^\dagger c_{1,A} - e^{-i\phi} c_{1,A}^\dagger c_{N,B}] \right\}, \quad (7)$$

where  $r$  and  $\phi$  are the amplitude and the phase of the hopping between the two ends of the chain, respectively.

In Fig. 3, we show how the energy spectrum is varying with  $\phi$  in a  $N = 6$  chain for several values of  $r$ . When  $r$  is relatively large, it still needs totally  $2N$  rounds to restore the initial sheet of the eigenvalues because each round shifts the adjacent energy levels one by one counterclockwise. When  $r$  is smaller than a critical value,  $r < r'_c$ , the circular alternation splits into three parts, in which two side ones include  $N - 1$  states and the center one has two states. So one will need  $2(N - 1)$  rounds to reach the initial spectrum sheet when  $N$  is an even number or  $(N - 1)$  rounds when  $N$  is odd. When  $r$  is further decreased to 0, which corresponds to the chain with OBC, the three circles shrink to three points at  $\pm 0.5$  and 0, respectively. So  $r = 0$  is also an EP of the Hamiltonian in the real space. But the degeneracy of this EP is smaller than that in the above toy model. Actually, there are totally three EPs that are overlapping with each other at

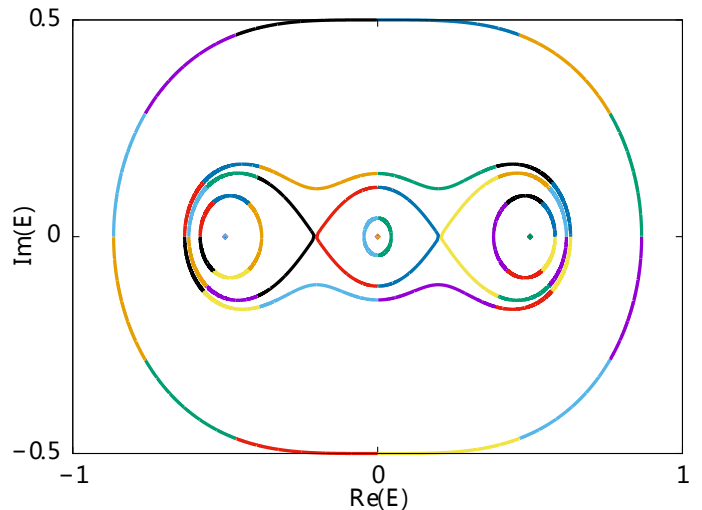


FIG. 3. (a) The traces in different colors show how are the eigenvalues evolving when  $\phi = 0 \rightarrow 2\pi$ . From outside to the inside,  $r$  is taking  $0.5$ ,  $1 \times 10^{-3}$ ,  $5.23 \times 10^{-4}$ ,  $6 \times 10^{-5}$  and  $0$ , respectively. When  $r = r_c = 5.23 \times 10^{-4}$ , the Hamiltonian encounters an EP at which two pairs of eigenvalues coalesce. As further decreasing  $r$ , the alternation of eigenvalues splits into three unconnected loops. When  $r = 0$ , there is another EP at where the eigenvalues coalesce to three points,  $0$  and  $\pm 0.5$ . Here the length of the chain is  $N = 6$ . Enlarging the chain does not change the evolution qualitatively, but  $r_c$  will exponentially decrease to  $0$ .

$r = 0$ , whose degeneracies are  $N - 1$ ,  $2$  and  $N - 1$ , respectively. One should remember that there is also another EP at  $(r = r'_c, \phi = \pi)$ , where two pairs of eigenvalues coalesce.

We also calculate the evolution of the spectrum for longer chains. The circular alternations are similar to those in the short chain presented in the above figure but the EP at  $r = r'_c$  is exponentially rapidly moved to the EP at the origin as the length of the chain is increased.

We plot the results when the parameters are changed to  $\gamma = 1$ ,  $v = -0.6$  and  $r_0 = 0.5$  in Fig. 4(a). In this case, the center EPs at  $r = 0$  is split into many EPs and are moved away from the origin. As Fig. 4(a) shows, when  $r$  is decreased to  $0.001$ , one EP has been encountered and the traces of eigenvalues are split into three parts with a center large loop containing 10 eigenvalues and the two satellite circles each containing 1 eigenvalue. As further decreasing  $r$ , more EPs are encountered and more and more eigenvalues are segregated from the center circle. When  $r = r_c = 3 \times 10^{-5}$ , the last two eigenvalues at the center coalesce. As all eigenvalues evolve to themselves when  $r < r_c$ , there is no EP anymore. So in this model,  $r = 0$  is not an EP and there are only two bound states near the zero energy when the OBC is finally reached. But when the length of the chain is increased to  $N = 20$ , whose results have been shown in Fig. 4(b), all EPs shrink toward 0 rapidly. The last two adherent eigenvalues coalesce at a much smaller  $r_c \sim 5.3 \times 10^{-15}$  and stay more close to the zero energy when  $r = 0$ . So we can conclude that even

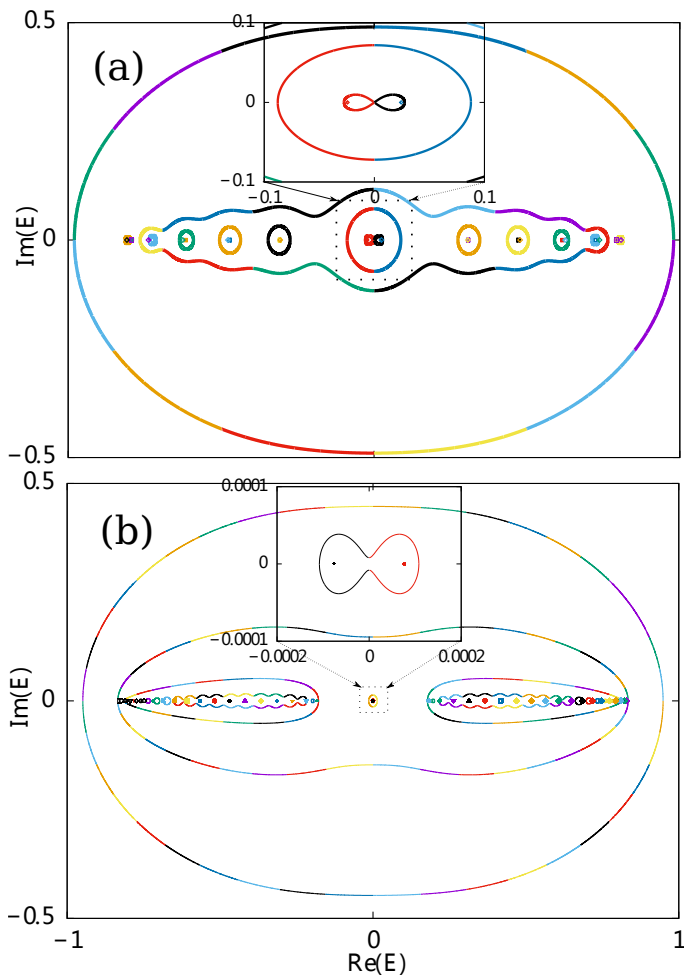


FIG. 4. (a) The traces of the eigenvalues when the parameters are changed to  $\gamma = 1$ ,  $v = -0.6$  and  $r_0 = 0.5$  in Eq. 7. Here from outside to the inside,  $r$  is taking  $0.5$ ,  $1 \times 10^{-3}$ ,  $5 \times 10^{-4}$ ,  $3.2 \times 10^{-5}$  and  $0$ , respectively. A zoom of the original region is shown in the inset. The length of the chain is still  $N = 6$ . (b) The traces of the eigenvalues when the length of the chain is changed to  $N = 20$ . Here  $r$  is taking  $0.5$ ,  $1 \times 10^{-6}$ ,  $1 \times 10^{-9}$ ,  $1 \times 10^{-10}$ ,  $5.3 \times 10^{-15}$  and  $0$ , respectively. The inset shows the mini circle and the saturate points when  $r = 5.3 \times 10^{-15}$  and  $0$ .

$r = 0$  is not an EP in this case, all EPs are moving toward it exponentially rapidly with enlarging the system.

The 2-dimensional(2D) model in Ref. 8 reads as

$$H_k = B_x(k_x, k_y)\sigma_z + B_y(k_x, k_y)\sigma_x, \quad (8)$$

where  $k_x$  and  $k_y$  are the wave-vectors in the  $x$  and  $y$  directions, respectively. Although this is a 2D model, the authors had considered  $k_y$  as a parameter and characterize the topological property by the fractional winding number in the  $k_x$  direction. So this model will be equivalent to the previous model in Eq. 6 from the topological side of the view.

### III. DISCUSSIONS

In real space representation, when the translational symmetry is restored by taking the amplitude of the hopping between the ends equal to that in bulk,  $r = r_0$ , the variation of  $\phi$  by  $2\pi$  is equivalent to the shift of the wave-vector  $k$  by  $\frac{2\pi}{N}$  in the Brillouin zone. As the period of the energy spectrum with  $k$  is  $4\pi$  in the momentum space, their period with  $\phi$  in the real space must be  $4N\pi$  instead of  $2N\pi$ . So on the complex plane ( $r \cos(\phi), r \sin(\phi)$ ), there must have several EPs inside the circle  $|re^{i\phi}| = r_0$ . For Eq. 7 with  $\gamma = 1$ ,  $v = -0.5$  and  $r_0 = 0.5$ , after writing down the Hamiltonian matrix with OBC,  $r = 0$ , one can immediately realize that this is an EP and there are at least two eigenvalues coalesce to zero energy. We suggest to attribute this ZEBS to the EP instead to the topological protected boundary state correspondent to the bulk fractional winding numbers for the following reasons.

Firstly, as we mentioned previously, the spectrum of the models with OBC or with periodic boundary condition are sharply different. All the states, including the ZEBS, are exponentially localized at the boundary in the former case, but are extended in the latter case. This distinction makes the two systems uncorrelated so that the topological numbers defined in the latter system has nothing to do with the spectrum when the OBC is taken.

Secondly, the fractional winding number defined in the momentum space is stemmed from the  $4\pi$  period of  $k$ . In real space, it has been inherited by the  $4N\pi$  period of  $\phi$  when  $r = r_0$ . So we can conclude that the topological number (fractional winding number here) is encoded in the topology of the traces of the eigenvalues. To reach OBC as decreasing  $r$ , one must encounter EPs and the topology of the traces must be changed (as one large loop splits into smaller loops shown in the previous figures). So it is impossible to associate the ZEBS at the open boundary to the fractional winding number defined without boundary because the topologies of the two systems are entirely different.

Thirdly, the ZEBSs are not protected by the chiral symmetry. They are actually caused by the fact that the Hamiltonian matrix with OBC has two eigenvalues coalesce to zero energy or near the zero energy. Taking Eq. 6 with the parameters  $\gamma = 1$ ,  $v = -0.5$  and  $r_0 = 0.5$  as an example, we can destroy this EP at  $r = 0$  by adding the term  $h(c_{1A}^\dagger c_{1A} - c_{NB}^\dagger c_{NB})$ , where  $h$  is a nonzero parameter. One should note that this term only alter the on-site energies in the two boundary unit cells but not the Hamiltonian in bulk. So if the ZEBSs are protected by the winding number defined in the bulk of the chain, they will mostly not be altered by the above extra term. But our numerical calculation indicates that the above term destroys the ZEBSs. We can further support our conclusion from another route. The definition of the winding number in the momentum space requires a chiral symmetry, which is  $\sigma_z H_k \sigma_z = -H_k$  in this article. If the topological understanding of ZEBS is right, they must

disappear when a term  $h\sigma_z$  is added in the Hamiltonian in Eq. 6. In the real space representation, we recover the EP at  $r = 0$  by eliminating the term  $h(c_{1A}^\dagger c_{1A} - c_{NB}^\dagger c_{NB})$  in the two unit cells at the boundaries. A simple numerical calculation confirms that the ZEBSs are still present. So even when there is no chiral symmetry and the fractional winding number is undefined, as long as the EP at  $r = 0$  is still present, the ZEBSs can still exist.

This article questions the topological understanding of ZEBS in NH models. But we are not challenging most of the results in Ref. 8 because the authors was discussing domain-walls instead of free boundaries there. Unlike the models with open boundaries, a system with domain-walls will not encounter the EP problem. But we want to emphasize that their conclusions on the domain-walls can not be further extended to the free boundaries. For instance, the index theorem in that article starts from a translation  $H' = H^\dagger H$  that maps the NH Hamiltonian  $H$  to an hermitian Hamiltonian  $H'$ . When  $H$  is not defective, the above translation maps the spectrum  $\epsilon$  to  $|\epsilon|^2$  one by one. But the Hamiltonian  $H$  will be defective right at the EP so that the spectrum of  $H'$  are not mapped one by one to that of  $H$  any more. The toy model in Eq. 1 can illustrate this: the eigenvalues of  $H^\dagger H$  are not fixed at zero when  $r_0 = 0$ . So the index theorem cannot be applied to the chain with OBC.

#### IV. CONCLUSIONS

We indicate that, as eliminating the amplitude of hopping between the ends of a chain to reach OBC, EP must be passed through and the topological structure of the band has been changed. This makes it impossible to associate the ZEBS in the OBC case to the fractional winding number defined without taking into account the boundary effect. The topological index theorem on a domain-wall cannot be naturally extended to that on the boundary for the same reason. The spectrum of the chain with OBC should be studied individually and the topological bulk boundary correspondence is cut out. Our studies also show that there are EP at or exponentially adjacent to  $r = 0$  in a long chain in these models. This makes it possible to study the effect of EP on a long chain without finely tune the parameters.

*Technical note:* Near or at the EP, the LU decomposition used by the lapack subroutines, i.e., zgeev is not stable. So it will give a wrong spectrum when the length of the chain is larger than 100 typically. We use a bi-orthogonal Gram-Schmidt process to calculate the spectrum in that case.

- 
- \* xiongye@njnu.edu.cn
- <sup>1</sup> A. Bohm, A. Mostafazadeh, H. Koizumi, Q. Niu, and J. Zwanziger, *The Geometric Phase in Quantum Systems* (Springer-Verlag Berlin Heidelberg, 2003).
  - <sup>2</sup> J. Gong and Q.-h. Wang, *Physical Review A* **82**, 012103 (2010).
  - <sup>3</sup> A. A. Mailybaev, O. N. Kirillov, and A. P. Seyranian, *Physical Review A* **72**, 014104 (2005), 0501040.
  - <sup>4</sup> M. S. Rudner and L. S. Levitov, *Physical Review Letters* **102**, 065703 (2009).
  - <sup>5</sup> K. Esaki, M. Sato, K. Hasebe, and M. Kohmoto, *Physical Review B* **84**, 205128 (2011).
  - <sup>6</sup> J. M. Zeuner, M. C. Rechtsman, Y. Plotnik, Y. Lumer, S. Nolte, M. S. Rudner, M. Segev, and A. Szameit, *Physical Review Letters* **115**, 040402 (2015).
  - <sup>7</sup> T. E. Lee, *Physical Review Letters* **116**, 133903 (2016).
  - <sup>8</sup> D. Leykam, K. Y. Bliokh, C. Huang, Y. D. Chong, and F. Nori, *Physical Review Letters* **118**, 040401 (2017).
  - <sup>9</sup> Y. C. Hu and T. L. Hughes, *Phys. Rev. B* **84**, 153101 (2011).
  - <sup>10</sup> N. Moiseyev, *Non-Hermitian Quantum Mechanics* (Cambridge University Press, Cambridge, England, 2011).
  - <sup>11</sup> M. Berry, *Czechoslovak Journal of Physics* **54**, 1039 (2004).
  - <sup>12</sup> W. D. Heiss, *JPhys A* **45**, 444016 (2012).
  - <sup>13</sup> H. Mehri-Dehnavi and A. Mostafazadeh, *Journal of Mathematical Physics* **49** (2008).
  - <sup>14</sup> S.-D. Liang and G.-Y. Huang, *Physical Review A* **87**, 012118 (2013).
  - <sup>15</sup> S. Malzard, C. Poli, and H. Schomerus, *Physical Review Letters* **115**, 200402 (2015).
  - <sup>16</sup> A. Cerjan, A. Raman, and S. Fan, *Physical Review Letters* **116**, 203902 (2016).
  - <sup>17</sup> Z. Lin, A. Pick, M. Lončar, and A. W. Rodriguez, *Physical Review Letters* **117**, 107402 (2016).
  - <sup>18</sup> Y. Xu, S.-T. Wang, and L.-M. Duan, *Physical Review Letters* **118**, 045701 (2017).
  - <sup>19</sup> W. Heisenberg, *Rev. Mod. Phys.* **29**, 269 (1957).
  - <sup>20</sup> C. M. Bender and S. Boettcher, *Physical Review Letters* **80**, 5243 (1998).
  - <sup>21</sup> C. M. Bender, D. C. Brody, and H. F. Jones, *Physical Review Letters* **89**, 270401 (2002).
  - <sup>22</sup> A. Mostafazadeh, *Journal of Mathematical Physics* **43**, 3944 (2002).
  - <sup>23</sup> X.-D. Cui and Y. Zheng, *Physical Review A* **86**, 064104 (2012).
  - <sup>24</sup> Y.-C. Lee, M.-h. Hsieh, S. T. Flammia, and R.-k. Lee, *Physical Review Letters* **112**, 130404 (2014).
  - <sup>25</sup> M. V. Medvedyeva, F. H. L. Essler, and T. Prosen, *Physical Review Letters* **117**, 137202 (2016).
  - <sup>26</sup> A. Amir, N. Hatano, and D. R. Nelson, *Physical Review E* **93**, 042310 (2016).
  - <sup>27</sup> G. Dattoli, R. Mignani, and A. Torre, *Journal of Physics A: Mathematical and General* **23**, 5795 (1990).
  - <sup>28</sup> M. Müller and I. Rotter, *Physical Review A - Atomic, Molecular, and Optical Physics* **80** (2009).
  - <sup>29</sup> R. El-Ganainy, K. G. Makris, D. N. Christodoulides, and Z. H. Musslimani, *Opt. Lett.* **32**, 2632 (2007).
  - <sup>30</sup> X.-D. Cui and Y. Zheng, *Scientific Reports* **4**, 5813 (2014).
  - <sup>31</sup> T. E. Lee and C.-k. Chan, *Physical Review X* **4**, 041001 (2014).

- <sup>32</sup> C. M. Bender, D. W. Hook, N. E. Mavromatos, and S. Sarkar, *Physical Review Letters* **113**, 231605 (2014).
- <sup>33</sup> T. Shah, R. Chattopadhyay, K. Vaidya, and S. Chakraborty, *Physical Review E* **92**, 062927 (2015).
- <sup>34</sup> S. Nixon and J. Yang, *Physical Review A* **93**, 031802 (2016).
- <sup>35</sup> A. Ruschhaupt, F. Delgado, and J. G. Muga, *Journal of Physics A: Mathematical and General* **38**, L171 (2005).
- <sup>36</sup> K. G. Makris, R. El-Ganainy, D. N. Christodoulides, and Z. H. Musslimani, *Phys. Rev. Lett.* **100**, 103904 (2008).
- <sup>37</sup> A. Guo, G. J. Salamo, D. Duchesne, R. Morandotti, M. Volatier-Ravat, V. Aimez, G. A. Siviloglou, and D. N. Christodoulides, *Phys. Rev. Lett.* **103**, 093902 (2009).
- <sup>38</sup> S. Longhi, *Phys. Rev. A* **82**, 031801 (2010).
- <sup>39</sup> S. Longhi, *Phys. Rev. Lett.* **103**, 123601 (2009).
- <sup>40</sup> C. E. Rüter, K. G. Makris, R. El-Ganainy, D. N. Christodoulides, M. Segev, and D. Kip, *Nature Physics* **6**, 192 (2010).
- <sup>41</sup> H. Ramezani, T. Kottos, R. El-Ganainy, and D. N. Christodoulides, *Phys. Rev. A* **82**, 043803 (2010).
- <sup>42</sup> Z. Lin, H. Ramezani, T. Eichelkraut, T. Kottos, H. Cao, and D. N. Christodoulides, *Phys. Rev. Lett.* **106**, 213901 (2011).
- <sup>43</sup> Z. Lin, J. Schindler, F. M. Ellis, and T. Kottos, *Phys. Rev. A* **85**, 050101 (2012).
- <sup>44</sup> N. Bender, S. Factor, J. D. Bodyfelt, H. Ramezani, D. N. Christodoulides, F. M. Ellis, and T. Kottos, *Phys. Rev. Lett.* **110**, 234101 (2013).
- <sup>45</sup> R. Fleury, D. L. Sounas, and A. Alù, *Phys. Rev. Lett.* **113**, 023903 (2014).
- <sup>46</sup> A. Regensburger, M.-A. Miri, C. Bersch, J. Näger, G. Onishchukov, D. N. Christodoulides, and U. Peschel, *Physical Review Letters* **110**, 223902 (2013).
- <sup>47</sup> Z. Zhang, Y. Zhang, J. Sheng, L. Yang, M.-a. Miri, D. N. Christodoulides, B. He, Y. Zhang, and M. Xiao, *Physical Review Letters* **117**, 123601 (2016).
- <sup>48</sup> H. Hodaei, M.-a. Miri, M. Heinrich, D. N. Christodoulides, and M. Khajavikhan, *Science* **975** (2014).
- <sup>49</sup> X. Zhu, H. Ramezani, C. Shi, J. Zhu, and X. Zhang, *Phys. Rev. X* **4**, 031042 (2014).
- <sup>50</sup> R. Fleury, D. Sounas, and A. Alù, *Nature Communications* **6**, 5905 (2015).
- <sup>51</sup> P.-Y. Chen and J. Jung, *Physical Review Applied* **5**, 064018 (2016).
- <sup>52</sup> Y. Xiong and P. Tong, ArXiv:1702.07112.
- <sup>53</sup> Y. Xiong, T. Wang, X. wang, and P. Tong, Arxiv:1610.06275.
- <sup>54</sup> Y. Xiong and P. Tong, *Journal of Statistical Mechanics: Theory and Experiment* , P02013 (2015)